

An Experimental Study of ILP Formulations for the Longest Induced Path Problem

Fritz Bökler^[0000-0002-7950-6965], Markus Chimani^[0000-0002-4681-5550],
 Mirko H. Wagner^[0000-0003-4593-8740], and Tilo Wiedera^[0000-0002-5923-4114]

Theoretical Computer Science, Osnabrück University, Germany
 {fboekler,markus.chimani,mirwagner,tilo.wiedera}@uni-osnabrueck.de

Abstract. Given a graph $G = (V, E)$, the LONGESTINDUCEDPATH problem asks for a maximum cardinality node subset $W \subseteq V$ such that the graph induced by W is a path. It is a long established problem with applications, e.g., in network analysis. We propose novel integer linear programming (ILP) formulations for the problem and discuss efficient implementations thereof. Comparing them with known formulations from literature, we prove that they are beneficial in theory, yielding stronger relaxations. Moreover, our experiments show their practical superiority.

1 Introduction

Let $G = (V, E)$ be an undirected graph and $W \subseteq V$. The W -induced graph $G[W]$ contains exactly the nodes W and those edges of G whose incident nodes are both in W . If $G[W]$ is a path, it is called an *induced path*. The length of a longest induced path is also referred to as the *induced detour number* which was introduced more than 30 years ago [8]. We denote the problem of finding such a path by LONGESTINDUCEDPATH. It is known to be NP-complete, even on bipartite graphs [17].

The LONGESTINDUCEDPATH problem has applications in molecular physics, the analysis of social, telecommunication, and more general transportation networks [3, 7, 25, 32] as well as pure graph and complexity theory: It is closely related to the graph *diameter*—the longest among all shortest paths between any two nodes, which is a commonly analyzed communication property of social networks [29]. A longest induced path witnesses the largest diameter that may occur by the deletion of any node subset in a node failure scenario [29]. The *tree-depth* of a graph is the minimum depth over all of its depth-first-search trees, and constitutes an upper bound on its treewidth [6], which is a well-established measure in parameterized complexity and graph theory. Recently, it was shown that any graph class with bounded degree has bounded induced detour number iff it has bounded tree-depth [31]. Further, the enumeration of induced paths can be used to predict nuclear magnetic resonance [35].

LONGESTINDUCEDPATH is not only NP-complete, but also W[2]-complete [9] and does not allow a polynomial $\mathcal{O}(|V|^{1/2-\epsilon})$ -approximation, unless $\text{NP} = \text{ZPP}$ [5, 24]. On the positive side, it can be solved in polynomial time for several graph

classes, e.g., those of bounded mim-width (which includes interval, bi-interval, circular arc, and permutation graphs) [26] as well as k -bounded-hole, interval-filament, and other decomposable graphs [18]. Furthermore, there are NP-complete problems, such as k -COLORING for $k \geq 5$ [22] and INDEPENDENT SET [28], are polynomial time solvable on graphs with bounded induced detour number.

Recently the first non-trivial, general algorithms to solve the LONGESTINDUCEDPATH problem exactly were devised by Matsypura et al. [29]. There, three different integer linear programming (ILP) formulations were proposed: the first searches for a subgraph with largest diameter; the second utilizes properties derived from the average distance between two nodes of a subgraph; the third models the path as a walk in which no shortcuts can be taken. Matsypura et al. show that the latter (see below for details) is the most effective in practice.

Contribution. In Section 3, we propose novel ILP formulations based on cut and subtour elimination constraints. We obtain strictly stronger relaxations than those proposed in [29] and describe a way to strengthen them even further in Section 4. After discussing some algorithmic considerations in Section 5, we show in Section 6 that our most effective models are also superior in practice.

2 Preliminaries

Notation. For $k \in \mathbb{N}$, let $[k] := \{0, \dots, k - 1\}$. Throughout this paper, we consider a connected, undirected, simple graph $G = (V, E)$ as our input. Edges are cardinality-two subsets of V . If there is no ambiguity, we may write uv for an edge $\{u, v\}$. Given a graph H , we refer to its nodes (edges) by $V(H)$ ($E(H)$, respectively). Given a cycle C in G , a *chord* is an edge connecting two nodes of $V(C)$ that are not neighbors along C .

Linear programming (cf., e.g., [34]). A *linear program* (LP) consists of a cost vector $c \in \mathbb{R}^d$ together with a set of linear inequalities, called *constraints*, that define a polyhedron \mathcal{P} in \mathbb{R}^d . We want to find a point $x \in \mathcal{P}$ that maximizes the *objective function* $c^\top x$. This can be done in polynomial time. Unless $P = NP$, this is no longer true when restricting x to have integral components; the so-modified problem is an *integer linear program* (ILP). Conversely, the *LP relaxation* of an ILP is obtained by dropping the integrality constraints on the components of x . The optimal value of an LP relaxation is a dual bound on the ILP’s objective; e.g., an upper bound for maximization problems. As there are several ways to *model* a given problem as an ILP, one aims for models that yield small dimensions and strong dual bounds, to achieve good practical performance. This is crucial, as ILP solvers are based on a branch-and-bound scheme that relies on iteratively solving LP relaxations to obtain dual bounds on the ILP’s objective. When a model contains too many constraints, it is often sufficient to use only a reasonably sized constraint subset to achieve provably optimal solutions. This allows us to add constraints during the solving process, which

is called *separation*. We say that model A is *at least as strong* as model B , if for all instances, the LP relaxation’s value of model A is no further from the ILP optimum than that of B . If there also exists an instance for which A ’s LP relaxation yields a tighter bound than that of B , then A is *stronger* than B .

When referring to models, we use the prefix “ILP” with an appropriate subscript. When referring to their respective LP relaxations we write “LP” instead.

Walk-based model (state-of-the-art). Recently Matsypura et al. [29] proposed an ILP model, ILP_{Walk} , that is the foundation of the fastest known exact algorithm (called **A3c** therein) for **LONGESTINDUCEDPATH**. They introduce timesteps, and for every node v and timestep t they introduce a variable that is 1 iff v is visited at time t . Constraints guarantee that nodes at non-consecutive time points cannot be adjacent. We recapitulate details in Appendix A. Unfortunately, ILP_{Walk} yields only weak LP relaxations (cf. [29] and Section 4). To achieve a practical algorithm, Matsypura et al. iteratively solve ILP_{Walk} for an increasing number of timesteps until the path found does not use all timesteps, i.e., a non-trivial dual bound is encountered. In contrast to [29], we consider the number of edges in the path (instead of nodes) as the objective value.

3 New Models

We aim for models that exhibit stronger LP relaxations and are practically solvable via single ILP computations. To this end, we consider what we deem a more natural variable space. We start by describing a partial model ILP_{Base} , which by itself is not sufficient but constitutes the core of our new models. To obtain a full model, ILP_{Cut} , we add constraints that prevent subtours.

For notational simplicity, we augment G to $G^* := (V^* := V \cup \{s\}, E^* := E \cup \{sv\}_{v \in V})$ by adding a new node s that is adjacent to all nodes of V . Within G^* , we look for a longest induced cycle through s , where we ignore induced chords incident to s . Searching for a cycle instead of a path, allows us to homogeneously require that each *selected* edge, i.e., edge in the solution, has exactly two adjacent edges that are also selected. Let $\delta^*(e) \subset E^*$ denote the edges adjacent to edge e in G^* . Each binary x_e -variable is 1 iff edge e is selected. We denote the partial model below by ILP_{Base} :

$$\max \sum_{e \in E} x_e \tag{1a}$$

$$\text{s.t. } \sum_{v \in V} x_{sv} = 2 \tag{1b}$$

$$2x_e \leq \sum_{f \in \delta^*(e)} x_f \leq 2 \quad \forall e \in E \tag{1c}$$

$$x_e \in \{0, 1\} \quad \forall e \in E^* \tag{1d}$$

Constraint (1b) requires to select exactly two edges incident with s . To prevent chords, constraints (1c) enforce that any (original) edge $e \in E$ (even if not selected itself!) is adjacent to at most two selected edges; if e is selected, precisely two of its adjacent edges need to be selected as well.

Establishing connectivity. The above model is not sufficient: it allows for the solution to consist of multiple disjoint cycles, only one of which contains s . But still, these cycles have no chords in G , and no edge in G connects any two cycles. To obtain a longest single cycle C through s —yielding the longest induced path $G[V(C) \setminus \{s\}]$ —we thus have to forbid additional cycles in the solutions that are not containing s . In other words, we want to enforce that the graph induced by the x -variables is connected.

There are several established ways to achieve connectivity: To stay with *compact* (i.e., polynomially sized) models, we could, e.g., augment ILP_{Base} with Miller-Tucker-Zemlin constraints (which are known to be polyhedrally weak [4]) or multi-commodity-flow formulations (ILP_{Flow} ; cf. Appendix B). However, herein we focus on augmenting ILP_{Base} with *cut* or (*generalized*) *subtour elimination* constraints, resulting in the (non-compact) model we denote by ILP_{Cut} , see below for details. Such constraints are a cornerstone of many algorithms for diverse problems where they are typically superior (in particular in practice) than other known approaches [15, 16, 33]. While ILP_{Cut} and ILP_{Flow} are polyhedrally equally strong (cf. Section 4), we know from other problems that the sheer size of the latter typically nullifies the potential benefit of its compactness. Preliminary experiments show that this is indeed the case here as well.

Cut model (and generalized subtour elimination). Let $\delta^*(W) := \{w\bar{w} \in E^* \mid w \in W, \bar{w} \in V^* \setminus W\}$ be the set of edges in the cut induced by $W \subseteq V^*$. For notational simplicity, we may omit braces when referring to node sets of cardinality one. We obtain ILP_{Cut} by adding *cut constraints* to ILP_{Base} :

$$\sum_{e \in \delta^*(v)} x_e \leq \sum_{e \in \delta^*(W)} x_e \quad \forall W \subseteq V, v \in W \quad (2a)$$

These constraints ensure that if a node v is incident to a selected edge (by (1c) there are then two such selected edges), any cut separating v from s contains at least two selected edges, as well. Thus, there are (at least) two edge-disjoint paths between v and s selected. Together with the cycle properties of ILP_{Base} , we can deduce that all selected edges form a common cycle through s .

An alternative view leads to *subtour elimination constraints* $\sum_{e \in E: e \subseteq W} x_e \leq |W| - 1$ for $W \subseteq V$, which prohibit cycles not containing s via counting. It is well known that these constraints can be generalized using binary node variables $y_v := \frac{1}{2} \sum_{e \in \delta^*(v)} x_e$ that indicate whether node $v \in V$ participates in the solution (in our case: in the induced path) [20]. *Generalized subtour elimination constraints* thus take the form

$$\sum_{e \in E: e \subseteq W} x_e \leq \sum_{w \in W \setminus \{v\}} y_w \quad \forall W \subseteq V, v \in W. \quad (2b)$$

One expects ILP_{Cut} and “ ILP_{Base} with constraints (2b)” to be equally strong as this is well-known for standard Steiner tree, and other related models [11, 12, 21]. In fact, there even is a direct one-to-one correspondence between cut constraints (2a) and generalized subtour elimination constraints (2b): By substituting node-variables with their definitions in (2b), we obtain $2 \sum_{e \in E: e \subseteq W} x_e \leq$

$\sum_{w \in W \setminus \{v\}} \sum_{e \in \delta^*(v)} x_e$. A simple rearrangement yields the corresponding cut constraint (2a).

Clique constraints. We further strengthen our above models by introducing a set of additional inequalities. Consider any clique (i.e., complete subgraph) in G . The induced path may contain at most one of its edges:

$$\sum_{e \in E: e \subseteq Q} x_e \leq 1 \quad \forall Q \subseteq V: G[Q] \text{ is a clique} \quad (3)$$

4 Polyhedral Properties of the LP Relaxations

We compare the above models w.r.t. the strength of their LP relaxations, i.e., the quality of their dual bounds. Achieving strong dual bounds is a highly relevant goal also in practice: one can expect a lower running time for the ILP solvers in case of better dual bounds since fewer nodes of the underlying branch-and-bound tree have to be explored. We defer the proofs of this section to Appendix C.

Since ILP_{Walk} requires *some* upper bound T on the objective value, we can only reasonably compare this model to ours by assuming that we are also given this bound as an explicit constraint. Hence, no dual bound of any of the considered models gives a worse (i.e., larger) bound than T . As has already been observed in [29], LP_{Walk} in fact *always* yields this worst case bound:

Proposition 1. (Proposition 5 from [29]) *For every instance and every number $T + 1 \leq |V|$ of timesteps LP_{Walk} has objective value T .*

Note that Proposition 1 is independent of the graph. Given that the longest induced path of a complete graph has length 1, we also see that the integrality gap of ILP_{Walk} is unbounded. Furthermore, this shows that ILP_{Base} cannot be weaker than ILP_{Walk} . We show that already the partial model ILP_{Base} is in fact *stronger* than ILP_{Walk} . Let therefore $\theta := T - \text{OPT} \in \mathbb{N}$, where OPT is the instance's (integral) optimum value.

Proposition 2. *ILP_{Base} is stronger than ILP_{Walk} . Moreover, for every $\theta \geq 1$ there is an infinite family of instances on which LP_{Base} has objective value at most $\text{OPT} + 1$ and LP_{Walk} has objective value at least $T = \text{OPT} + \theta$.*

Since ILP_{Cut} only has additional constraints compared to ILP_{Base} , this implies that ILP_{Cut} is also stronger than ILP_{Walk} . In fact, since constraints (2a) cut off infeasible integral points contained in ILP_{Base} , LP_{Cut} is clearly even a strict subset of LP_{Base} . As noted before, we can show that using a multi-commodity-flow scheme (cf. Appendix B) results in LP relaxations equivalent to LP_{Cut} :

Proposition 3. *ILP_{Flow} and ILP_{Cut} are equally strong.*

Let $\text{ILP}_{\text{Cut}}^k$ denote ILP_{Cut} with clique constraints added for all cliques on at most k nodes. We show that increasing the clique sizes yields a hierarchy of ever stronger models.

Proposition 4. *For any $k \geq 4$, $\text{ILP}_{\text{Cut}}^k$ is stronger than $\text{ILP}_{\text{Cut}}^{k-1}$.*

5 Algorithmic Considerations

Separation. Since ILP_{Cut} contains an exponential number of cut constraints (2a), it is not practical in its full form. We follow the traditional separation pattern for branch-and-cut-based ILP solvers: We initially omit cut constraints (2a), i.e., we start with model $M := \text{ILP}_{\text{Base}}$. Iteratively, given a feasible solution to the LP relaxation of M , we seek violated cut constraints and add them to M . If no such constraints are found and the solution is integral, we have obtained a solution to ILP_{Cut} . Otherwise, we proceed by branching or—given a sophisticated branch-and-cut framework—by more general techniques.

Given an LP solution \hat{x} , we call an edge $e \in E$ *active* if $\hat{x}_e > 0$. Similarly, we say that a node is *active*, if it has an active incident edge. These active graph elements yield a subgraph H of G^* . For integral LP solutions, we simply compute the connected components of H and add a cut constraint for each component that does not contain s . We refer to this routine as *integral separation*. For a fractional LP solution, we compute the maximum flow value f_v between s and each active node v in H ; the capacity of an edge $e \in E^*$ is equal to \hat{x}_e . If $f_v < \sum_{e \in \delta^*(v)} \hat{x}_e$, a cut constraint based on the induced minimum s - v -cut is added. We call this routine *fractional separation*. Both routines manage to find a violated constraint if there is any, i.e., they are *exact* separation routines. In fact, this shows that an optimal solution to LP_{Cut} can be computed in polynomial time [23]. Note that already integral separation suffices to obtain an exact, correct algorithm—we simply may need more branching steps than with fractional separation.

Relaxing variables. As presented above, our models have $\Theta(|E|)$ binary variables, each of which may be used for branching by the ILP solver. We can reduce this number, by introducing $\Theta(|V|)$ new binary variables y_v , $v \in V$, that allow us to relax the binary x_e -variables, $e \in E$, to continuous ones. The new variables are precisely those discussed w.r.t. generalized subtour elimination, i.e., we require $y_v = \frac{1}{2} \sum_{e \in \delta^*(v)} x_e$. Assuming x_e to be continuous in $[0, 1]$, we have for every edge $e = \{v, w\} \in E$: if $y_v = 0$ or $y_w = 0$ then $x_e = 0$. Conversely, if $y_v = y_w = 1$ then $x_e = 1$ by (1c). Hence, requiring integrality for the y -variables (and, e.g., branching only on them), suffices to ensure integral x values.

Handling clique constraints. We use a modified version of the Bron-Kerbosch algorithm [14] to list all maximal cliques. For each such clique we add a constraint during the construction of our model. Recall that there are up to $3^{n/3}$ maximal cliques [30], but preliminary tests show that this effort is negligible compared to solving the ILP. Thus, as our preliminary tests also show, other (heuristic) approaches of adding clique constraints to the initial model are not worthwhile.

6 Computational Experiments

Algorithms. We implement the best state-of-the-art algorithm, i.e., the ILP_{Walk} -based one by Matsypura et al. as briefly described in Section 2 and Appendix A.

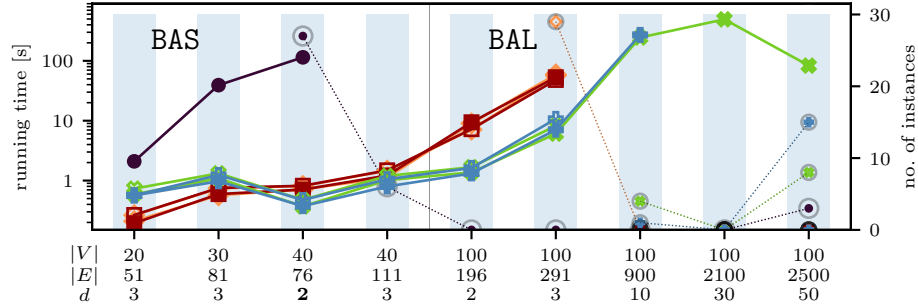
We denote this algorithm by “W”. For our implementations of ILP_{Cut} , we consider various parameter settings w.r.t. to the algorithmic considerations described in Section 5. We denote the arising algorithms by “C” to which we attach sub- and superscripts defining the parameters: the subscript “frac” denotes that we use fractional separation in addition to integral separation. The superscript “n” specifies that we introduce node variables as the sole integer variables. The superscript “c” specifies that we use clique constraints. We consider all eight thereby possible ILP_{Cut} implementations.

Hard- and software. Our C++ (GCC 8.3.0) code uses SCIP 6.0.1 [19] as the Branch-and-Cut-Framework with CPLEX 12.9.0 as the LP solver. We use OGDF snapshot-2018-03-28 [10], in particular its push-relabel implementation, for the separation of cut constraints. We use igraph 0.7.1 [13] to calculate all maximal cliques. For W, we directly use CPLEX instead of SCIP as the Branch-and-Cut-Framework. This does not give an advantage to our algorithms, since CPLEX is more than twice as fast as SCIP [1] and we confirmed in preliminary tests that CPLEX is faster on ILP_{Walk} . However, we use SCIP for our algorithms, as it allows better parameterizable user-defined separation routines. We run all tests on an Intel Xeon Gold 6134 with 3.2 GHz and 256 GB RAM running Debian 9. We limit each test instance to a single thread with a time limit of 20 minutes and a memory limit of 8 GB.

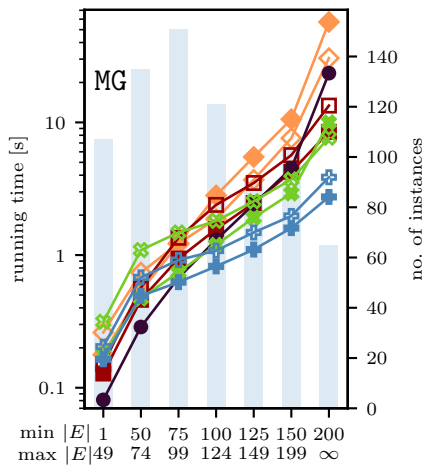
Instances. We consider the instances proposed for $\text{LONGESTINDUCEDPATH}$ in [29] as well as additional ones. Overall, our test instances are grouped into four sets: RWC, MG, BAS and BAL. The first set, denoted RWC, is a collection of 22 real-world networks, including communication and social networks of companies and of characters in books, as well as transportation, biological, and technical networks. See [29] for details on the selection. The *Movie Galaxy* (MG) set consists of 773 graphs representing social networks of movie characters [27]. While [29] considered only 17 of them, we use the full set here. The other two sets are based on the Barabási-Albert probabilistic model for scale-free networks [2]. In [29], only the chosen parameter values are reported, not the actual instances. Our set BAS recreates instances with the same values: 30 graphs for each choice $(|V|, d) \in \{(20, 3), (30, 3), (40, 3), (40, 2)\}$, where $d = \frac{|E|+1}{|V|}$ is the graph’s density. As we will see, these small instances are rather easy for our models. We thus also consider a set BAL of graphs on 100 nodes; for each density $d \in \{2, 3, 10, 30, 50\}$ we generate 30 instances. See <http://tcs.uos.de/research/lip> for all instances, their sources, and detailed experimental results.

Comparison to the state-of-the-art. We start with the most obvious question: Are the new models practically more effective than the state-of-the-art? See Fig. 1a for BAS and BAL, Fig. 1b for MG, and Table 1 for RWC.

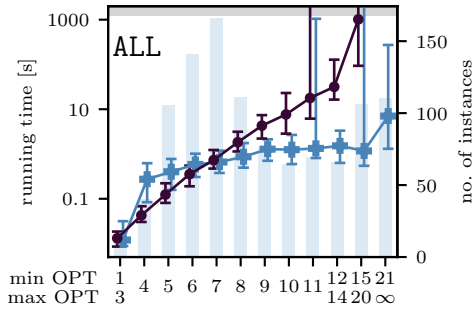
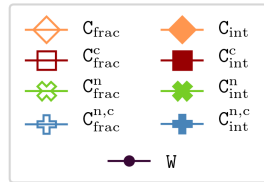
We observe that rather independent of the benchmark set, the various ILP_{Cut} implementations achieve the best running times and success rates. The only



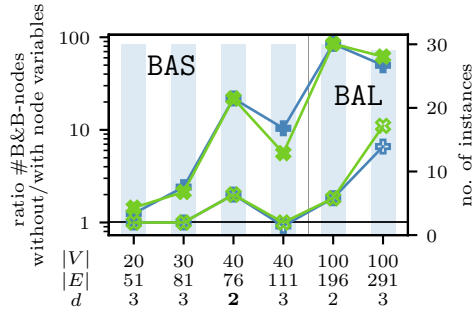
(a) Running time on BAS and BAL



(b) Running time on MG



(c) Running time vs. OPT (all instances)



(d) Reduction of B&B-nodes by node var's on commonly solved BAS and BAL

Fig. 1: Comparison between different ILP models.

(a),(b): Each point is a median, where timeouts are treated as ∞ seconds. Bars in the background give the number of instances. Gray encircled markers, connected via dotted lines, show the number of solved instances (if not 100%).

(c): Whiskers mark the 20% and 80% percentile. The gray area marks timeouts.

Table 1: Running times [s] on RWC except for **yeast** and **622bus** (solved by none). We denote timeouts by \ominus and mark times within 5% of the minimum in bold.

instance	OPT	V	E	W	C _{int}	C _{frac}	C _{int} ^c	C _{frac} ^c	C _{int} ⁿ	C _{frac} ⁿ	C _{int} ^{n,c}	C _{frac} ^{n,c}
high-tech	13	33	91	15.40	0.90	1.11	1.44	3.15	0.51	0.81	0.41	2.05
karate	9	34	78	2.98	1.73	1.65	2.12	1.32	1.07	3.71	0.66	2.74
mexican	16	35	117	73.30	1.68	2.25	1.12	3.59	1.22	1.34	0.87	0.99
sawmill	18	36	62	70.00	0.51	0.43	0.50	0.44	0.85	3.32	0.82	3.34
taylorS1	13	39	158	83.80	4.78	7.92	4.81	6.45	1.51	1.87	3.29	3.55
chesapeake	16	39	170	106.00	1.84	13.11	2.11	11.00	2.29	4.88	3.19	4.39
taylorS2	15	39	223	445.00	6.80	21.78	11.92	14.91	3.20	4.31	2.89	3.14
attiro	31	59	128	\ominus	1.76	2.57	2.48	1.75	1.20	1.75	0.89	1.19
krebs	17	62	153	522.00	3.86	28.21	18.55	10.03	16.00	11.26	3.90	2.33
dolphins	24	62	159	\ominus	7.95	27.59	22.72	18.33	19.21	2.99	3.01	4.70
prison	36	67	142	\ominus	13.36	5.87	1.09	1.50	3.62	4.05	1.02	1.02
huck	9	69	297	41.70	\ominus	144.13	19.46	42.22	114.27	11.63	5.96	7.49
sanjuansur	38	75	144	\ominus	30.67	8.64	24.86	10.33	8.22	3.65	3.79	4.71
jean	11	77	254	121.00	464.89	52.89	16.54	9.53	81.03	14.47	3.88	5.14
david	19	87	406	\ominus	666.25	719.46	26.70	45.34	85.88	23.94	6.93	10.35
ieeebus	47	118	179	\ominus	37.10	22.35	39.82	10.60	15.69	3.13	22.72	5.61
sfi	13	118	200	44.40	47.41	4.39	4.89	3.77	15.13	2.64	3.31	2.44
anna	20	138	493	\ominus	21.58	296.69	53.21	74.55	439.23	20.27	7.09	7.58
usair	46	332	2126	\ominus	\ominus	\ominus	\ominus	\ominus	\ominus	\ominus	922.94	\ominus
494bus	142	494	586	\ominus	\ominus	379.29	\ominus	379.97	\ominus	178.92	\ominus	170.74

exceptions are the instances from MG (cf. Fig. 1b): there, the overhead of the stronger model, requiring an explicit separation routine, does not pay off and W yields comparable performance to the weaker of the cut-based variants. On BAS instances, the cut-based variants dominate (cf. Fig. 1a): while all variants (see below) solve all of BAS, W can only solve the instances for $d \in \{20, 30\}$ reliably. On BAL (cf. Fig. 1a) W fails on virtually all instances. The cut-based model, however, allows implementations (see below for details) that solve all of these harder instances. We point out one peculiarity on the BAL instances, visible in Fig. 1a. The instances have 100 nodes but varying density. As the density increases from 2 to 30, the median running times of all algorithmic variants increase and the median success rates decrease. However, from $d = 30$ to $d = 50$ (where only C_{int}ⁿ is successful) the running times drop again and the success rate increases. Interestingly, the number of branch-and-bound (B&B) nodes for $d = 50$ is only roughly 1/7 of those for $d = 30$. This suggests that the denser graphs may allow fewer (near-)optimal solutions and thus more efficient pruning of the search tree.

Comparison of cut-based implementations. Choosing the best among the eight ILP_{Cut} implementations is not as clear as the general choice of ILP_{Cut} over ILP_{Walk}. In Fig. 1a, 1b, and Table 1 we see that, while adding clique constraints is clearly beneficial on MG, on BAS and RWC the benefit is less clear. On BAL, we do not see a benefit and for $d \in \{30, 50\}$ we even see a clear benefit of *not* using clique constraints. Each of the graphs from BAL with $d \in \{30, 50\}$ has at least 4541 maximal cliques—and therefore initial clique constraints—, whereas the BAL graphs for $d = 10$ and the RWC graphs **yeast** and **usair** have at most 581 maximal cliques and all other graphs have at most 102.

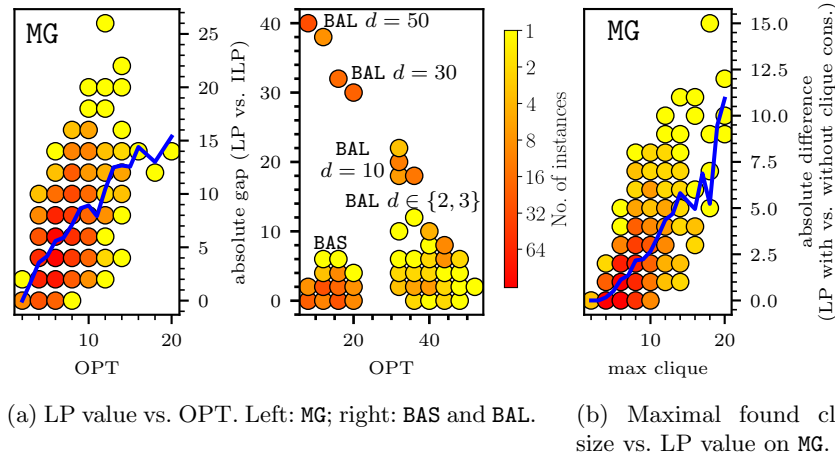


Fig. 2: Root LP relaxation of cut-based models. The blue line shows the median.

The probably most surprising finding is the choice of the separation routine: while the fractional variant is a quite fast algorithm and yields tighter dual bounds, the simpler integral separation performs better in practice. This is in stark contrast to seemingly similar scenarios like TSP or Steiner problems, where the former is considered by default. In our case, the latter—being very fast and called more rarely—is seemingly strong enough to find effective cutting planes that allow the ILP solver to achieve its computations fastest. This is particularly true when combined with the addition of node variables (see below). In fact, C_{int}^n is the only choice that can completely solve all large graphs in BAL.

Adding node variables (and relaxing the integrality on the edge variables) nearly always pays off significantly (cf. Fig. 1a, 1b). Fig. 1d shows that the models without node variables require many more B&B-nodes. In fact, looking more deeply into the data, C_{int}^n requires roughly as few B&B-nodes as C_{frac} without requiring the overhead of the more expensive separation routine. Only for BAS with $|V| \in \{20, 30\}$, the configurations without node variables are faster; on these instances, our algorithms only require 2–6.5 B&B-nodes (median).

Dependency of running time on the optimal value. Since the instances optimal value OPT determines the final size of the ILP_{Walk} instance, it is natural to expect the running time of W to heavily depend on OPT. Fig. 1c shows that this is indeed the case. The new models are less dependent on the solution size, as, e.g., witnessed by $C_{\text{int}}^{n,c}$ in the same figure.

Practical strength of the root relaxations. For our new models, we may ask how the integer optimal solution value and the value of the LP relaxation (obtained by any cut-based implementation with exact fractional separation) differ, see Fig. 2a. The gap increases for larger values of OPT. Interestingly, we

observe that the *density* of the instance seems to play an important role: for **BAS** and **BAL**, the plot shows obvious clusters, which—without a single exception—directly correspond to the different parameter settings as labeled. Denser graphs lead to weaker LP bounds in general.

Fig. 2b shows the relative improvement to the LP relaxation when adding clique constraints for **MG** instances. On the other hand for every instance of **BAS** and **BAL** the root relaxation did not change by adding clique constraints.

7 Conclusion

We propose new ILP models for **LONGESTINDUCEDPATH** and prove that they yield stronger relaxations in theory than the previous state-of-the-art. Moreover, we show that they—generally, but also in particular in conjunction with further algorithmic considerations—clearly outperform all known approaches in practice. We also provide strengthening inequalities based on cliques in the graph and prove that they form a hierarchy when increasing the size of the cliques.

It could be worthwhile to separate the proposed clique constraints (at least heuristically) to take advantage of their theoretical properties without overloading the initial model with too many such constraints. As it is unclear how to develop an *efficient* such separation scheme, we leave it as future research.

References

1. Achterberg, T.: SCIP: solving constraint integer programs. *Math. Prog. Comput.* **1**(1), 1–41 (2009)
2. Barabasi, A.L., Albert, R.: Emergence of Scaling in Random Networks. *Science* **286**, 509–512 (1999)
3. Barabasi, A.L.: *Network Science*. Cambridge University Press (2016)
4. Bekta, T., Gouveia, L.: Requiem for the Miller-Tucker-Zemlin subtour elimination constraints? *EJOR* **236**(3), 820–832 (2014)
5. Berman, P., Schnitger, G.: On the Complexity of Approximating the Independent Set Problem. *Inf. Comput.* **96**(1), 77–94 (1992)
6. Bodlaender, H.L., Gilbert, J.R., Hafsteinsson, H., Kloks, T.: Approximating Treewidth, Pathwidth, Frontsize, and Shortest Elimination Tree. *J. Alg.* **18**(2), 238–255 (1995)
7. Borgatti, S.P., Everett, M.G., Johnson, J.C.: *Analyzing Social Networks*. SAGE Publishing (2013)
8. Buckley, F., Harary, F.: On longest induced paths in graphs. *Chinese Quart. J. Math.* **3**(3), 61–65 (1988)
9. Chen, Y., Flum, J.: On Parameterized Path and Chordless Path Problems. In: *CCC*. pp. 250–263 (2007)
10. Chimani, M., Gutwenger, C., Juenger, M., Klau, G.W., Klein, K., Mutzel, P.: The Open Graph Drawing Framework (OGDF). In: Tamassia, R. (ed.) *Handbook on Graph Drawing and Visualization*, pp. 543–569. Chapman and Hall/CRC (2013), www.ogdf.net
11. Chimani, M., Kandyba, M., Ljubić, I., Mutzel, P.: Obtaining Optimal k -cardinality Trees Fast. *J. Exp. Alg.* **14**, 5:2.5–5:2.23 (2010)

12. Chimani, M., Kandyba, M., Ljubić, I., Mutzel, P.: Strong Formulations for 2-Node-Connected Steiner Network Problems. In: COCOA. pp. 190–200. LNCS 5165 (2008)
13. Csardi, G., Nepusz, T.: The igraph software package for complex network research. *InterJournal, Complex Systems* **1695**, 1–9 (2006), <http://igraph.sf.net>
14. Eppstein, D., Löffler, M., Strash, D.: Listing All Maximal Cliques in Sparse Graphs in Near-Optimal Time. In: ISAAC. pp. 403–414. LNCS 6506 (2010)
15. Fischetti, M.: Facets of two Steiner arborescence polyhedra. *Math. Prog.* **51**, 401–419 (1991)
16. Fischetti, M., Salazar-Gonzalez, J., Toth, P.: The Generalized Traveling Salesman and Orienteering Problems. In: *The Traveling Salesman Problem and Its Variations*, Comb. Opt., vol. 12. Springer (2007)
17. Garey, M.R., Johnson, D.S.: *Computers and Intractability: A Guide to the Theory of NP-Completeness*. W. H. Freeman & Co. (1979)
18. Gavril, F.: Algorithms for maximum weight induced paths. *Inf. Process. Let.* **81**(4), 203–208 (2002)
19. Gleixner, A., Bastubbe, M., Eifler, L., Gally, T., Gamrath, G., Gottwald, R.L., Hendel, G., Hojny, C., Koch, T., Lübbecke, M.E., Maher, S.J., Miltenberger, M., Müller, B., Pfetsch, M.E., Puchert, C., Rehfeldt, D., Schlösser, F., Schubert, C., Serrano, F., Shinano, Y., Viernickel, J.M., Walter, M., Wegscheider, F., Witt, J.T., Witzig, J.: *The SCIP Optimization Suite 6.0*. ZIB-Report 18-26, Zuse Inst. Berlin (2018), <https://scip.zib.de>
20. Goemans, M.X.: The steiner tree polytope and related polyhedra. *Math. Prog.* **63**, 157–182 (1994)
21. Goemans, M.X., soo Myung, Y.: A Catalog of Steiner Tree Formulations. *Networks* **23**, 19–28 (1993)
22. Golovach, P.A., Paulusma, D., Song, J.: Coloring graphs without short cycles and long induced paths. *Disc. Appl. Math.* **167**, 107–120 (2014)
23. Grötschel, M., Lovász, L., Schrijver, A.: *Geometric Algorithms and Combinatorial Optimization*, Alg. and Comb., vol. 2. Springer (1988)
24. Håstad, J.: Clique is hard to approximate within $n^{1-\epsilon}$. *Acta Math.* **182**(1), 105–142 (1999)
25. Jackson, M.O.: *Social and Economic Networks*. Princeton University Press (2010)
26. Jaffke, L., Kwon, O., Telle, J.A.: Polynomial-Time Algorithms for the Longest Induced Path and Induced Disjoint Paths Problems on Graphs of Bounded Mim-Width. In: IPEC. pp. 21:1–13. LIPIcs 89 (2017)
27. Kaminski, J., Schober, M., Albaladejo, R., Zastupailo, O., Hidalgo, C.: *Moviegalleries - Social Networks in Movies*. Harvard Dataverse (V3 2018)
28. Lozin, V., Rautenbach, D.: Some results on graphs without long induced paths. *Inf. Process. Let.* **88**(4), 167–171 (2003)
29. Matsypura, D., Veremyev, A., Prokopyev, O.A., Pasiliao, E.L.: On exact solution approaches for the longest induced path problem. *EJOR* **278**, 546–562 (2019)
30. Moon, J.W., Moser, L.: On Cliques in Graphs. *Israel J. of Math.* **3**(1), 23–28 (1965)
31. Nešetřil, J., de Mendez, P.O.: *Sparsity - Graphs, Structures, and Algorithms*, Alg. and Comb., vol. 28. Springer (2012)
32. Newman, M.: *Networks: An Introduction*. Oxford University Press (2010)
33. Polzin, T.: *Algorithms for the Steiner problem in networks*. Ph.D. thesis, Saarland University, Saarbrücken, Germany (2003)
34. Schrijver, A.: *Theory of linear and integer programming*. Wiley-Intersci. series in disc. math. and opt., Wiley (1999)
35. Uno, T., Satoh, H.: An Efficient Algorithm for Enumerating Chordless Cycles and Chordless Paths. In: *Int. Conf. on Disc. Sci.* pp. 313–324. LNCS 8777 (2014)

APPENDIX

A Walk-Based Model (State-of-the-Art)

The following ILP model, denoted by ILP_{Walk} , was recently presented in [29]. It constitutes the foundation of the fastest known exact algorithm. It models a timed walk through the graph that prevents “short-cut” edges. Let T denote an upper bound on the length of the path, i.e., on its number of edges. For every node $v \in V$ and every point in time $t \in [T + 1]$ there is a variable x_v^t that is 1 iff v is visited at time t (4g).

$$\max \quad \sum_{t=1}^T \sum_{v \in V} x_v^t \quad (4a)$$

$$\text{s.t.} \quad \sum_{v \in V} x_v^t \leq 1 \quad \forall t \in [T + 1] \quad (4b)$$

$$\sum_{t=0}^T x_v^t \leq 1 \quad \forall v \in V \quad (4c)$$

$$\sum_{v \in V} x_v^{t+1} \leq \sum_{v \in V} x_v^t \quad \forall t \in [T] \quad (4d)$$

$$x_v^t \leq 1 - \sum_{w \in V: vw \notin E} x_w^{t+1} \quad \forall v \in V, t \in [T] \quad (4e)$$

$$x_v^t \leq 1 - \sum_{\tau=t+2}^T x_w^\tau \quad \forall vw \in E, t \in [T - 1] \quad (4f)$$

$$x_v^t \in \{0, 1\} \quad \forall v \in V, t \in [T + 1] \quad (4g)$$

In every step at most one node can be visited (4b); a node can be visited at most once (4c); the time points have to be used consecutively (4d); nodes visited at consecutive time points need to be adjacent (4e); and nodes at non-consecutive time points cannot be adjacent (4f).

However, ILP_{Walk} yields only weak LP relaxations (cf. Section 4). To obtain a practical algorithm, the authors of [29] iteratively solve ILP_{Walk} for increasing values of T until its optimal objective value becomes less than T . They use the graph’s diameter as a lower bound on T to avoid trivial calls. In addition, they add supplemental symmetry breaking inequalities.

B Multi-Commodity-Flow Model

A flow formulation allows a *compact*, i.e., polynomially-sized, model. We start with ILP_{Base} and extend it in the following way: Each node $v \in V$ is assigned a commodity and sends—if v is part of the induced path—two units of flow of this commodity from v to s using only selected edges, where edges have capacity one (per commodity). This ensures that each node in the solution lies on a common cycle with s . Consider the bidirected arc set $A^* := \{(vw), (wv) \mid \{v, w\} \in E^*\}$ that consists of a directed arc for both directions of each edge in E^* . Let $\delta_{\text{out}}^*(v)$ ($\delta_{\text{in}}^*(v)$) denote the arcs of A^* with source (resp. target) $v \in V$. We use variables

z_a^v to model the flow of commodity v over arc $a \in A^*$; we do not actively require them to be binary. The below model, together with ILP_{Base} , forms ILP_{Flow} .

$$z_{(uw)}^v \leq x_{\{u,w\}} \quad \forall v \in V, (uw) \in A^* \quad (5a)$$

$$\sum_{a \in \delta_{\text{out}}^*(w)} z_a^v = \sum_{a \in \delta_{\text{in}}^*(w)} z_a^v + \mathbb{1}_{w=v} \cdot \sum_{e \in \delta^*(v)} x_e \quad \forall w, v \in V \quad (5b)$$

$$0 \leq z_a^v \leq 1 \quad \forall v \in V, a \in A^* \quad (5c)$$

The capacity constraints (5a) ensure that flow is only sent over selected edges. Equations (5b) model flow preservation (up to, but not including, the sink s) and send the commodities away from their source v , if v is part of the solution.

C Proofs for Section 4 (Polyhedral Properties)

Proposition 1. (Proposition 5 from [29]) *For every instance and every number $T + 1 \leq |V|$ of timesteps LP_{Walk} has objective value T .*

Proof. We set x_v^t to $1/|V|$ for all $v \in V$ and $t \in [T + 1]$. It is easy to see that this solution is feasible and attains the claimed objective value. \square

Proposition 2. *ILP_{Base} is stronger than ILP_{Walk} . Moreover, for every $\theta \geq 1$ there is an infinite family of instances on which LP_{Base} has objective value at most $\text{OPT} + 1$ and LP_{Walk} has objective value at least $T = \text{OPT} + \theta$.*

Proof. By Proposition 1, LP_{Walk} will always attain value $T = \text{OPT} + \theta$. To show the strength claim, it thus suffices to give instances where LP_{Base} yields a strictly tighter bound.

Already a star with at least three leaves proves the claim, as LP_{Base} guarantees a solution of optimal value 2. However, it can be argued that such graphs and substructures are easy to preprocess. Thus, we prove the claim with a more suitable instance class.

Choose any $\ell \geq 3$, start with two nodes v_L, v_R , connect them with ℓ internally node-disjoint paths of length 2, and add new node v' with edge $v_R v'$. A longest induced path in this graph contains exactly 3 edges: $v_R v'$ and the two edges of one of the v_L - v_R -paths. Let $\deg(v) := |\{e \in E : v \in E\}|$ denote the degree of node v in G without added star s . By summing all constraints (1c) we deduce

$$2|E| \geq \sum_{e \in E} \sum_{f \in \delta^*(e)} x_f \geq \underbrace{\sum_{e \in E} \sum_{f \in \delta^*(e) \cap E} x_f}_a + \underbrace{\sum_{v \in V} \deg(v) \cdot x_{sv}}_b.$$

For the double sum a we see that any edge incident to v_L or v' is considered ℓ times, i.e., it has ℓ adjacent edges, while the other edges are considered $\ell + 1$ times. Thus $a \geq \ell \sum_{e \in E} x_e$. In the second sum b , $v_R v'$ is the only edge with coefficient 1 (instead of ≥ 2), and we thus have $b \geq (2 \sum_{v \in V} x_{sv}) - x_{sv'}$. By (1b) and the variable bounds we have $b \geq 4 - 1 = 3$. Since $|E| = 2\ell + 1$ we overall

have $2(2\ell + 1) \geq \ell \sum_{e \in E} x_e + 3$, giving objective value $\sum_{e \in E} x_e \leq 4 - \frac{1}{\ell}$. As the objective must be integral, this even yields the optimal bound 3 when using LP_{Base} within an ILP solver.

We furthermore note that, to achieve strictly two-connected graphs, we could, e.g., also consider a cycle where each edge is replaced by two internally node-disjoint paths of length 2. However, in the above instance class the gap between the relaxations is larger, which is why we refrain from giving further details to the latter class. \square

Proposition 3. ILP_{Flow} and ILP_{Cut} are equally strong.

Proof. Let \mathcal{P}_{Cut} and $\mathcal{P}_{\text{Flow}}$ be the polytope of LP_{Cut} and LP_{Flow} , respectively. Let $\mathcal{P}'_{\text{Flow}}$ be the projection of $\mathcal{P}_{\text{Flow}}$ onto the x -variables by ignoring the z -variables. Then $\mathcal{P}_{\text{Cut}} = \mathcal{P}'_{\text{Flow}}$. We show that the projection is surjective. Clearly, it retains the objective value. We observe that by constraints (5a) for any node v there can be at most x_e units of flow along edge e that belong to some commodity v . By constraint (5b), each node $v \in V$ sends $\sum_{e \in \delta^*(v)} x_e$ units of flow that have to arrive at node s . Consequently, the claim—both that any LP_{Flow} solution maps to an LP_{Cut} solution and vice versa—follows directly from the duality of max-flow and min-cut. \square

Proposition 4. For any $k \geq 4$, $\text{ILP}_{\text{Cut}}^k$ is stronger than $\text{ILP}_{\text{Cut}}^{k-1}$.

Proof. $\text{ILP}_{\text{Cut}}^k$ is as least as strong as $\text{ILP}_{\text{Cut}}^{k-1}$ as we only add new constraints. Let $G = K_k$, the complete graph on k nodes. By choosing $Q = V$ in constraint (3), LP_{Cut}^k has objective value 1.

However, $\text{LP}_{\text{Cut}}^{k-1}$ allows a solution with objective value $\omega := 1 + \frac{2}{k-2} > 1$: We set $\tilde{x}_e := \omega / \binom{k}{2}$ for each $e \in E$ and $\tilde{x}_{sv} := \frac{2}{k}$ for each $v \in V$ to obtain an LP feasible solution \tilde{x} to $\text{LP}_{\text{Cut}}^{k-1}$: Clearly, constraints (1b,1c) are satisfied. The cut constraints (2a) are satisfied since edge variables are chosen uniformly (w.r.t. the two above edge types) and the right-hand side of the constraint sums over at least as many edge variables (per type) as the left-hand side. For any clique of size at most $k - 1$, the left-hand side of its clique constraint (3) sums up to at most $\binom{k-1}{2} \cdot \tilde{x}_e = \binom{k-1}{2} (1 + \frac{2}{k-2}) / \binom{k}{2} = 1$.

We note that it is straight-forward to generalize G , so that it contains K_k only as a subgraph, while retaining the property of having a gap between the two considered LPs. \square